DP-MS-78-31

IRRADIATION EFFECTS IN MAGNESIUM AND ALUMINUM ALLOYS

by

E. F. Sturcken

Savannah River Laboratory
E. I. du Pont de Nemours & Co.
Aiken, SC 29801

Proposed for Publication in the
Journal of Nuclear Materials

This document was prepared in conjunction with work accomplished under Contract No. DE-AC09-76SR00001 with the U.S. Department of Energy.

DISCLAIMER

IRRADIATION EFFECTS IN MAGNESIUM AND ALUMINUM ALLOYS

E. F. STURCKEN

Savannah River Laboratory, E. I. du Pont de Nemours and Co.,

Aiken, South Carolina 29801, USA

Effects of neutron irradiation on microstructure, mechanical properties, and swelling of several magnesium and aluminum alloys were studied. The neutron fluences of 2-3 x 10^{22} n/cm^2 > 0.2 Mev produced displacement doses of 20 to 45 displacements per atom (dpa).

Ductility of the magnesium alloys was severely reduced by irradiation induced recrystallization and precipitation of various forms. Precipitation of transmuted silicon occurred in the aluminum alloys. However, the effect on ductility was much less than for the magnesium alloys.

The magnesium and aluminum alloys had excellent resistance to swelling: The best magnesium alloy was Mg/3.0 wt% Al/0.19 wt% Ca; its density decreased by only 0.13%. The best aluminum alloy was 6063, with a density decrease of 0.22%.

IRRADIATION EFFECTS IN MAGNESIUM AND ALUMINUM ALLOYS

E. F. STURCKEN

Savannah River Laboratory, E. I. du Pont de Nemours and Co.,

Aiken, South Carolina 29801, USA

Introduction

Irradiation effects on structural materials are of considerable interest in predicting deterioration of mechanical properties and swelling in structural components used in fission and fusion reactor environments.

Irradiation effects in pure magnesium have been reported by Levy et al [1], Adda [2], Jostsons and Farrell [3], and Sturcken and Krapp [4]. For a fluence of 2×10^{21} n/cm.^{2} > 0.1 Mev the principle irradiation effects were hexagonal shaped voids and partial dislocations with their associated stacking faults. The degree of void swelling was greater than for pure aluminum, however, the voids were annealed out by heat treatment for 3.6 ks (1 hour) at 320°C. For higher fluences (2.6×10^{22} n/cm.^{2} > 0.1 Mev) the irradiation effects were more severe than for pure aluminum in several respects, fig. 1: a) Anisotropic distortion of the sample was severe; b) In addition to voids, intergranular cavities contributed to the overall swelling; c) Even though neutron collisions with atoms occur homogeneously throughout the sample, the

voids occurred in "swirling" patterns that varied extremely in density from one region to another within a single grain; and d) For heat treatments of 4 hrs. at 450°C most of the voids did not anneal out, but instead grew by an order of magnitude.

The observed irradiation effects in pure magnesium were postulated by Sturcken and Krapp [4] to be caused by the following mechanism: Atom displacements during irradiation cause layers of interstitials to precipitate on basal planes resulting in prismatic loops with Burgers vector $\underset{\sim}{b} = c/2\ [0001]$ containing high energy stacking faults with three violations of the next nearest neighbor rule. High energy faults transform to low energy faults through the nucleation of Shockley partials $\underset{\sim}{b} = a/3\ [10\bar{1}0]$ and subsequent interaction with $\underset{\sim}{b} = c/2\ [0001]$ to form low energy faults bounded by prismatic loops with Burgers vector $\underset{\sim}{b} = a/6\ [20\bar{2}3]$. This interaction causes a shearing of the lattice on the basal plane. Precipitation of interstitials leaves a supersaturation of vacancies which form voids on the basal planes. Since the voids form only on one set of planes, the grains deform anisotropically and thereby cause intergranular cavities and overall distortion. Extreme variation in void density occurs because vacancies are "swept out" in the regions containing fewer voids by the deformation associated with the lattice shearing on the basal planes. In a later paper [5] Jostsons and Farrell have used the same high energy fault nucleation and transformation mechanism to interpret their observations on the dislocation structure and annealing behavior of irradiated magnesium.

Irradiation effects in a magnesium alloy, Magnox Al 80 (Mg/0.8 wt% Al/0.005 wt% Be) have been reported by Eldred [6] and by Gibbs and Harris [7]. The alloy is used as a can for uranium fuel elements. Eldred [6] found that the creep ductility decreased with increasing radiation, and the decrease was attributed [7] to helium gas atoms generated from the ^{6}Li (n, α) reaction by trace amounts of lithium in the alloy.

Preliminary results indicating good swelling resistance for the alloy Mg/3.0 wt% Al/0.2 wt% Ca have been reported by Sturcken and Krapp [4], and further results will be given below. The alloying elements discussed in the present paper, namely Al, Ca, Ce, Sn, were chosen to have low neutron absorption cross sections and high neutron scattering factors.

Irradiation effects in aluminum and aluminum alloys have been reported by many authors [8-31]. The principle irradiation effects are dislocation networks, voids and silicon precipitates formed by the thermal neutron transmutation reaction $^{27}Al(n, \gamma)\ ^{28}Al$, $^{28}Al \xrightarrow{\beta^-} {}^{28}Si$. It is generally believed that the mechanism of void formation is vacancy supersaturation caused by precipitation of interstitial loops which grow rapidly into dislocation networks and act as biased sinks for interstitials. The characteristics of void formation as a function of irradiation and materials variables have been reviewed by Stiegler [8]. The degree of void swelling in aluminum is greatly reduced by alloying, and the most swelling resistant aluminum alloys are 6061 and 6063; the swelling resistance of

these alloys is attributed [25, 28] to the presence of the coherent precipitate, Mg_2 Si.

Transmutation produced silicon precipitates in aluminum, and the effect of the precipitates on mechanical properties has been discussed by Farrell et al [15], Jostons et al [14], King et al [25], and Sturcken and Krapp [28]. Mechanical property changes for the highest neutron fluences have been reported by King, Farrell, and Richt [29] and by Korth, Beeston, Martin, and Brinkman [27].

2. Experimental and Analytical Procedures

2.1 Magnesium and Aluminum Alloys

Magnesium alloys were cast as three inch diameter ingots by the permanent mold process using magnesium metal of greater than 99.7% purity. The ingots were homogenized for seven days at 416°C except for the Mg/3.0 wt% Al/0.19 wt% Ca ingot, which was homogenized seven days at 416°C and five days at 482°C. The ingots were removed directly from the furnace and hot extruded to 1.905 cm and 0.635 cm diameter rods. The 1.905 cm rods were used to prepare the specimen holders and the 0.635 cm rods to prepare the specimens. The samples were given a final heat treatment of 2 weeks at 200°C to stabilize them for the experimental operating temperature of 100 to 125°C. Chemical compositions of the magnesium and aluminum alloys are given in table 1.

The aluminum alloys studied were commercial alloys 1100 and 6063. They were specified as reactor grade which limits nuclear

poisons to a maximum weight percent of 0.001 boron, 0.003 cadmium, 0.001 cobalt, and 0.008 lithium. The 1100 alloy was tested in the strain hardened and fully annealed conditions. The 6063 alloy was tested in the solution heat treated, precipitation hardened, and overaged conditions.

2.2 Irradiation Conditions

The alloys were irradiated as rods and tensile samples (fig. 2) in position F-7 of the High Flux Isotope Reactor (HFIR) Target Bundle at ORNL for a total of 302.35 full power days (100 megawatts per day). Thermal and fast neutron fluences and irradiation temperatures are given in table 2.

The fluence data were furnished by T. M. Sims of ORNL from multigroup diffusion theory calculations supported by cobalt, gold, nickel, aluminum and magnesium foil activation data.

2.3 Measurements and Equipment

Microstructure, mechanical properties, density, and x-ray diffraction measurements were made on the samples before and after irradiation. The data reported for the tensile tests represent averages of three samples each.

Liquid displacement density measurements were made with a six-place Mettler balance using both relative [32] and absolute [33] methods. Diamond pyramid micro-hardness (DPH) measurements were made on a Tukon Hardness Tester using a 0.5 kg load and a dwell time of 15 seconds. An average of five identations was used for

each sample. The tensile specimens were tested on an Instron tester at room temperature at a strain rate of 0.05 cm per 60 seconds.

X-ray diffraction studies were performed on a Norelco diffractometer with a fine-focus CuKα x-ray tube and a graphite single crystal monchromator on the detector side of the diffractometer. Powder diffraction data were also obtained with a Debye-Scherrer camera. Scanning electron microscopy (SEM) was performed on an AMR-900 microscope and x-ray energy spectroscopy on a Kevex 5000A x-ray energy spectrometer.

Alloys were prepared for metallographic examination by wet grinding on a conventional horizontal polishing wheel with 240, 300, 400, and 600 grit silicon carbide paper. Magnesium alloys were polished with 600 grit *"Alundum,"* 0.3 micron alpha alumina, and 0.05 micron *"Magomet"* and etched with a solution of 10 ml acetic acid, 4.2g picric acid, 10 ml water, 70 ml ethanol (95%). Aluminum alloys were polished with 15, 6, and 1 micron diamond dust and 0.05 micron *"Magomet"* and etched with solutions of 1 g of NaOH in 100 ml water and 1 ml HF (48%) in 200 ml water.

3. Results and Discussion

3.1 Density Changes in Magnesium Alloys

Density changes for the magnesium alloys are shown in table 3. The changes were small and were the least, -0.13%, for the Mg/3.0 wt% Al/0.19 wt% Ca alloy.

The density changes were not caused by void swelling, but by precipitation of aluminum that was originally in substitutional solid solution in the magnesium lattice. The magnesium lattice is contracted in the unirradiated state, table 4, because of the presence of aluminum which has a smaller atomic diameter than magnesium. During irradiation the aluminum precipitates as $Al_{12}Mg_{17}$ which has a density of 2.068 g/cm.^{3} compared to magnesium, 1.738 g/cm.^{3}. The magnesium lattice expands, table 4, due to loss of the aluminum. The change in volume determined from the lattice parameter measurements before and after irradiation is greater than the actual volume change determined from the density measurements because the density measurements include the added volume of the precipitate.

The Mg/5.1 wt% Al/1.6 wt% Sn alloy had the greatest change in density, -0.51%, probably because in addition to $Al_{12}Mg_{17}$, it also formed the precipitate Mg_2Sn which has a density of 3.662 g/cm.^{3} and therefore contributed less volume.

As previously reported [4], pure magnesium metal had large decreases in density, -10.6%, due to the presence of hexagonal voids and intergranular cavities. The lattice was also expanded due to the presence of extrinsic stacking faults on the basal planes.

3.2 Density Changes in Aluminum Alloys

Density changes for the aluminum alloys are shown in table 3. The density change of the 1100 Al, -0.3%, compares well with that measured for 1100 Al by Jostsons and Long [13]. During irradiation

0.52 wt% Si was generated in the 1100 Al by nuclear transmutation. Silicon has a low solubility in aluminum, and it will precipitate. If all the Si were precipitated as metallic silicon, it would account for about ¼ of the observed density change. The density change was the same for the strain hardened and annealed tempers.

Even though the fluence was 50% greater, table 2, the 6063 Al had a smaller density change, -0.2%, than the 1100 Al. The amount of silicon generated was 0.76 wt%, which if present as metallic silicon, would account for about half of the observed density change. The density change in the 6063 Al was the same, table 3, for the solution heat treated, precipitation hardened, and overaged tempers.

3.3 Radiation Effects on Mechanical Properties

All of the alloys had the generally observed irradiation effects of increased yield and ultimate strength and hardness and decreased ductility, tables 5 and 6.

The magnesium alloys experienced severe losses in ductility. Two of the alloys, Mg/5.1 wt% Al/1.6 wt% Sn and Mg/5.2 wt% Al/0.2 wt% Ca fractured during tensile tests with less than 0.3% plastic elongation, and the other magnesium alloys retained only 2 to 3 percent total elongation to fracture. The cause of the embrittlement is believed to be irradiation induced precipitation and will be discussed in the section on irradiation effects on microstructure and fracture mode.

As might be expected, the aluminum alloys retained their properties much better than the magnesium alloys, table 5. However, they were very sensitive to initial temper. The 1100 Al with the annealed temper (DPH=27) lost more ductility and experienced greater hardness increases than the strain hardened temper. The 6063 Al with the overaged temper (DPH=30) lost more ductility and had greater hardness increases than the precipitation hardened tempers. However, for both alloys the "soft" tempers were still more ductile after irradiation. The principle effects causing the property changes were precipitated silicon and dislocation hardening. Voids were not observed.

3.4 Irradiation Effects on Microstructure and Fracture Mode

3.41 Magnesium Alloys

Prior to irradiation, the Mg/7.7 wt% Al alloy had some fine oriented precipitates in the grains and at the grain boundaries, fig. 3(a). However, most of the aluminum was in solid solution as evidenced by the lattice parameters, table 4. During irradiation the original precipitates dissolved, and a new precipitate structure developed, fig. 3(b). The lattice parameter after irradiation indicated that most of the aluminum had precipitated from solid solution to form $Al_{12}Mg_{17}$. The irradiation induced precipitate structure was similar to that produced [34] in Mg/8 wt% Al by solution heat treatment and aging and is believed to be formed by simultaneous recrystallization and precipitation of the equilibrium solute-rich phase at an advancing front throughout individual grains.

The precipitates, fig. 3(b), are long with very small diameters and are lightly curved rather than straight; as if they formed in flow patterns. Several flow patterns develop within a grain. Geisler [35] points out that the role of the recrystallization reaction during the precipitation process in metals is to provide a means for decreasing the free energy of the strained matrix. Turnbull [36] has suggested the term "cellular precipitation" for this phenomena.

Polycrystalline magnesium deforms [34] under room temperature tensile loading by basal and non-basal slip, twinning, and accommodation kinking and grain boundary shearing. The observed strain is contributed mostly by slip [4], while the other mechanisms operate to satisfy the requirements for continuity and to produce more favorable orientations for basal slip. After 3% strain, microcracks are usually observed at twins and grain boundaries.

Fracture surfaces of tensile specimens from irradiated and unirradiated Mg/7.7 wt% Al are shown in fig. 3(c) and 3(d). The fracture surface of the unirradiated tensile specimen has the general appearance of ductile intragranular fracture, however, one can see a few microcracks, and the grain boundaries are indicated by the different orientations of the undulations due to basal slip in adjoining grains. In contrast, the fracture surface of the irradiated tensile specimen has numerous microcracks, and the deformation appears to have occurred at the boundaries between the precipitate and the matrix (compare fig. 3(b) with fig. 3(d)).

Prior to irradiation,the Mg/5 wt% Al/0.35 wt% Ce alloy had

most of the aluminum in solid solution, however, a large number of aluminum-cerium precipitates were present, fig. 4(a), because the amount of cerium present exceeded the solid solubility of cerium in magnesium (0.15 wt% at 337°C). The aluminum-cerium precipitates did not appear to be affected by the irradiation. Aluminum precipitated during irradiation as $Al_{12}Mg_{17}$, which appeared partly with an oriented Widmanstätten structure and partly as cellular precipitation, fig. 4(b), similar to the flow patterns seen in the Mg/7.7 wt% Al alloy.

The unirradiated fracture surface, fig. 4(c), is characteristic of ductile intragranular failure with some holes caused by Al-Ce precipitates. The irradiated fracture surface, fig. 4(d), is also intragranular but has numerous microcracks, and the fracture is partly by cleavage on crystallographic planes and partly by deformation of the soft matrix regions from which cellular precipitations occurred.

Prior to irradiation, the Mg/5.1 wt% Al/1.6 wt% Sn had some oriented rod shaped precipitates of $Al_{12}Mg_{17}$ and some equiaxed precipitates of Mg_2Sn in the grains, fig. 5(a). During irradiation the precipitates were dissolved, and the large grain structure recrystallized into a finer grain structure with a fine Widmanstätten precipitate of $Al_{12}Mg_{17}$ within the grains and Mg_2Sn precipitates in the grain boundaries, fig. 5(b). There was no evidence of cellular precipitation in this alloy.

The large decrease in the grain size of the Mg/5.1 wt% Al/1.6 wt% Sn alloy after irradiation is seen in the fracture surfaces of

the tensile specimens before and after irradiation, figs. 6(a) and 6(b). Unirradiated Mg/5.1 wt% Al/1.6 wt% Sn tensile specimens fractured intragranularly, fig. 6(c), in a ductile manner similar to the other alloys, with a few more microcracks due to the larger grain size. Irradiated Mg/5.1 wt% Al/1.6 wt% Sn tensile specimens fractured at grain boundaries and within the grains. The fracture surface within the grains had undulations similar to those caused by basal slip in pure magnesium [4]. However, this tensile specimen fractured with only 0.3% elongation; therefore, the undulations are probably not due to slip but to cleavage on crystallographic planes. It is known from previous studies that $Al_{12}Mg_{17}$ precipitates on $\{11\bar{2}0\}$ and (0001), making these planes the least resistant to fracture. In addition, the orientation is favorable for maximum shear stress on (0001) and tensile stress on $(11\bar{2}0)$ in a number of grains because the samples were extruded and have the basal planes parallel to the axis of the tensile specimen. Furthermore, in the high magnification micrographs, fig. 6(d), the surfaces of the undulations are not smooth as in the unirradiated tensile specimens, but have small holes the size of the $Al_{12}Mg_{17}$ precipitates.

Prior to irradiation, the Mg/3.0 wt% Al/0.19 wt% Ca alloy had both very fine and large precipitates, fig. 7(a), of Al_2Ca throughout the grains because the calcium present exceeded the solid solubility of calcium in magnesium (0.1 wt% at 350°C). Most of the aluminum was in solid solution. This alloy had the smallest grain size; probably because of the very fine Al_2Ca precipitates. During irradiation the fine Al_2Ca precipitates dissolved, or became too small

to observe, and larger Al_2Ca particles appeared in the grain boundaries, fig. 7(b). At the same time, $Al_{12}Mg_{17}$ precipitated in the grains. The $Al_{12}Mg_{17}$ precipitates were so small that they could not be detected by a conventional x-ray diffraction powder pattern. However, a diffractometer trace of a large cross section of the tensile specimen gave small, very broad $Al_{12}Mg_{17}$ reflections for the (110), (332), (422), (331), and (550) planes. These reflections were detectable because the preferred orientation of the sample caused them to have increased diffraction intensity, and the {1120} planes of magnesium are common planes for $Al_{12}Mg_{17}$ precipitation. The polished and lightly etched surface of the grains have a sponge-like structure, fig. 7(b), not present in the unirradiated samples, which is believed to be the relief surface from which the fine precipitates were etched.

Fracture surfaces of unirradiated and irradiated Mg/3.0 wt% Al/0.19 wt% Ca are shown in fig. 7(c), 7(c). The unirradiated fracture surface had the general appearance of ductile intragranular rupture, and the grain size was so fine that grain boundaries were not delineated. The fracture surface of the irradiated specimen was totally intergranular with many microcracks between grains suggesting that most of the deformation was by grain boundary shearing.

Unirradiated Mg/5.2 wt% Al/0.2 wt% Ca had a larger grain size than the Mg/3.0 wt% Al/0.19 wt% Ca alloy and only relatively large Al_2Ca precipitates, fig. 8(a), in contrast to the fine Al_2Ca precipitates that were observed in Mg/3.0 wt% Al/0.19 wt% Ca alloy. These

fine precipitates were apparently produced by the higher temperature homogenizing heat treatment. Most of the aluminum was in solid solution. During irradiation $Al_{12}Mg_{17}$ precipitated with a Widmanstätten structure, fig. 8(b), in the grains. The large Al_2Ca particles remained in the grains. However, more Al_2Ca particles appeared in the grain boundaries.

Fracture surfaces of unirradiated and irradiated Mg/5.2 wt% Al/ 0.2 wt% Ca are shown in figs. 8(c) and 8(d). The unirradiated fracture surface shows ductile intragranular rupture. The irradiated fracture surface shows mostly intergranular fracture with undulations on the surface of some grains that are believed to be due to cleavage on crystallpgraphic planes. These specimens fractured at 0.3 per cent total elongation.

3.42 Aluminum Alloys

The composition of the 1100 aluminum alloy is shown in table 1. Because of the relatively low silicon content (<.06 wt%), most of the precipitates were Al_3Fe plus a few $Al_{12}Fe_3$ Si particles. There was very little Fe in the matrix. Some of the copper present (0.15 wt%) was in the matrix and some in the $Al_{12}Fe_3$ Si particles.

During irradiation 0.52 wt% Si was produced in the 1100 alloy by nuclear transmutation. Some of the silicon precipitated as fine particles in the matrix. In addition, most of the large precipitates were $Al_{12}Fe_3$ Si rather than Al_3Fe indicating that some of the transmuted Si had reacted with the Al_3Fe to form $Al_{12}Fe_3$ Si.

Fracture surfaces of tensile specimens from both unirradiated and irradiated 1100 aluminum showed intragranular ductile rupture.

The composition of the 6063 aluminum alloys is also shown in table 1. The solution treated and age hardened tempers have a fine needle like precipitate of Mg_2 Si in a Widmanstätten structure that is best observed with high resolution transmission electron microscopy [28]. Large Mg_2 Si particles in the overaged temper were also difficult to observe because they were easily attacked and etched out during polishing. The most frequently observed precipitates seen with optical and scanning electron microscopy were $Al_{12}Fe_3$ Si.

During irradiation 0.76 wt% Si was produced in the 6063 Al by nuclear transmutation and a fine precipitate, believed to be the Si (fig. 9), formed in the matrix. The large precipitates ($Al_{12}Fe_3$ Si) did not appear to change. It is possible that some changes also occurred in the Mg_2 Si precipitates. However, no TEM studies were made to look for such effects.

The principle effects of irradiation on the tensile fracture behavior of 6063 aluminum was to change the mode of fracture from totally intragranular to about 50% intergranular, figs. 10(a) and 10 (b). The same amount of intergranular fracture was produced by age hardening the unirradiated samples from DPH$\cong$60 to DPH$\cong$80.

4. Conclusions

The ductility of magnesium alloys, irradiated to high fluences, was severely reduced by irradiation induced precipitation and recrystallization of various forms that depended on the amount and

kind of alloying additions.

Alloys with the cellular precipitation of $Al_{12}Mg_{17}$ fractured intragranularly at the boundary between the matrix and the precipitate. Alloys with the Widmanstätten precipitate of $Al_{12}Mg_{17}$ in the grains and grain boundary precipitates of Al_2Ca and Mg_2Sn fractured intergranularly.

All of the alloying additions to magnesium eliminated swelling. However, the alloy with the lowest aluminum addition, Mg/3.0 wt% Al/ 0.19 wt% Ca, retained the most ductility. Even in this alloy it appeared that less aluminum (e.g., 1.0 wt% Al) and less calcium (e.g., 0.05 wt% Ca), to prevent grain boundary precipitation of Al_2Ca, would have been desirable. The alloy should also be homogenized at a relatively high temperature and time (e.g., 2 wks. at 500°C) to assure good grain refinement by forming very fine Al_2Ca precipitates.

Precipitation of transmuted silicon occurred in the aluminum alloys, but did not seriously reduce their ductility. The 6063 aluminum when irradiated to high hardness (e.g., DP=100) or age hardened in the absence of irradiation, changed its mode of fracture from completely intragranular to about 50% intergranular. Intergranular fracture was not associated with precipitates in the grain boundaries as was the case for the magnesium alloys. In addition, x-ray scans across the grain boundaries showed no concentration of silicon. It is believed the intergranular fracture occurred because the grains became sufficiently strengthened and limited in their modes of deformation by the fine Si precipitates that the required stress was

reached for grain boundary shear. The 6063 aluminum had excellent resistance to swelling.

Acknowledgements

The author is grateful to G. B. Alewine of the Savannah River Plant for her assistance in the design of the test assembly and the irradiation test, to C. W. Krapp of this laboratory for his assistance with the experimental measurements, and to the Oak Ridge Staff, especially Dr. R. T. King, R. C. Wier, and E. M. King for their assistance with the experiment.

REFERENCES

[1] V. Levy, J. Mathie, A. Risbet, R. Levy, and J. P. Poirer, Voids Formed by Irradiation of Reactor Materials, British Nuclear Energy Society, Reading, March 24-25, 1971, p. 63.

[2] Y. Adda, Proc. 1971 Int. Conf., Radiation-Induced Voids in Metals, State University of New York at Albany, June 9-11, 1971, p. 31.

[3] A. Jostsons and K. Farrell, radiat. eff., 8 (1971) 287.

[4] E. F. Sturcken and C. W. Krapp, Proceedings of the Fifth International Materials Symposium, Electron Microscopy and Structure of Materials. University of California, Berkeley, September 13-17, 1971, University of California Press, Berkeley, 1972, p. 996.

[5] A. Jostsons and K. Farrell, radiat. eff., 15 (1972) 217.

[6] V. W. Eldred, The Metallurgist, 3 (1964) 57.

[7] G. B. Gibbs and J. E. Harris, radiat. eff., 16 (1972) 267.

[8] J. O. Stiegler, ibid ref. [2] p. 292.

[9] A. Jostsons, E. L. Long, Jr., J. O. Stiegler, K. Farrell, and D. N. Braski, ibid ref. [2] p. 363.

[10] K. Farrell, T. T. Houston, A. Wolfenden, R. T. King, and A. Jostsons, ibid ref. [2] p. 376.

[11] H. D. Gronbeck, USAEC Report IN-1036 (1967).

[12] R. V. Steele and W. P. Wallace, USAEC, Report, LRL-145 (1954).

[13] A. Jostsons and E. L. Long, Jr., radiat. eff., 16 (1972) 83.

[14] A. Jostsons and R. T. King, Scr. Met., 6 (1972) 447.

[15] K. Farrell, J. O. Stiegler, and R. E. Gehlbach, Metallography, 3 (1970) 275.

[16] N. H. Packan, ibid ref. [1] p. 71

[17] N. H. Packan, J. Nucl. Mater. 40 (1971) 1.

[18] J. O. Stiegler, K. Farrell, C. K. H. DuBose, and R. T. King, Radiation Damage in Reactor Materials, Proc. IAEA Symp., Vienna 1969, Vol. 2 p. 215.

[19] K. Farrell, A. Wolfenden, and R. T. King, radiat. eff., 8 (1971) 107.

[20] K. Farrell and R. T. King, Phys. Stat. Sol., (a) 2 (1970) K5.

[21] R. T. King, E. L. Long, Jr., J. O. Stiegler, and K. Farrell, J. Nucl. Mater. 35 (1970) 231.

[22] N. H. Packan, J. Nucl. Mater. 37 (1970) 251.

[23] A. Wolfenden, J. Nucl. Mater. 40 (1971) 351.

[24] H. E. McCoy, Jr. and J. R. Weir, Jr., Nucl. Sci. Eng. 25 (1966) 319.

[25] R. T. King, A. Jostsons, and K. Farrell, Amer. Soc. Test. Mater., Spec. Tech. Publ. 529, p. 165.

[26] K. Farrell and R. T. King. Met. Trans. 4 (1973) 1223.

[27] G. E. Korth, J. M. Beeston, M. R. Martin, and C. R. Brinkman, Nuclear Metallurgy, Vol. 19, Symposium On Materials Performance In Operating Nuclear Systems, Ames Laboratory, Iowa State University, Ames, Iowa, August 28-30, 1973, USAEC CONF-730801, p. 88.

[28] E. F. Sturcken, C. W. Krapp, and G. B. Alewine, ibid ref. [27] p. 108.

[29] R. T. King, K. Farrell, and A. E. Richt, ibid ref. [27] p. 133.

[30] K. Farrell, R. T. King, A. Jostsons, and E. Long, Jr., ibid ref. [27] p. 153.

[31] K. Farrell and J. T. Houston, Proc. Int. Conf., Gatlinburg, Tenn., Oct. 1-3, 1975, Radiation Effects and Tritium Technology for Fusion Reactors, ORNL CONF-750989, Vol. II, p. 209.

[32] R. T. Ratcliffe, Brit. J. Appl. Phys., 16 (1965) 1193.

[33] H. A. Bowman and R. M. Schoonover, J. Res. NBS, 71C, No. 3, (1967) 179.

[34] C. S. Roberts, "Magnesium and Its Alloys," John Wiley and Sons, New York (1960) p. 121.

[35] A. H. Geisler in R. Smoluchowski, J. E. Mayer, and W. A. Weyl, "Phase Transformation In Solids," John Wiley and Sons, New York, (1951) p. 432.

[36] D. Turnbull, Acta Met. 3 (1955) 55.

Table 1

Composition Of Magnesium And Aluminum Alloys (wt.%)

	Pure Mg	Mg-Al	Mg-Al-Ca	Mg-Al-Ca	Mg-Al-Ce	Mg-Al-Sn	1100 Al	6063 Al
Al	0.002	7.7	3.0	5.2	5.0	5.1	Balance	Balance
Ca	<0.01	<0.01	0.19	0.20	<0.01	<0.01	-	-
Ce	-	-	-	-	0.35	-	-	-
Cu	<0.001	<0.001	<0.001	<0.001	<0.001	<0.001	0.13	0.01
Fe	0.001	0.004	0.001	0.003	0.005	<0.001	0.40	0.20
Mg	Balance	Balance	Balance	Balance	Balance	Balance	0.018	0.59
Mn	0.001	<0.01	0.003	<0.01	<0.01	<0.01	0.01	0.0075
Ni	<0.001	0.001	0.002	<0.001	0.001	0.001	0.007	0.002
Pb	<0.01	<0.01	<0.01	<0.01	<0.01	<0.01	0.0008	0.0003
Si	<0.005	<0.01	<0.005	<0.01	<0.01	<0.01	<0.06	0.39
Sn	<0.005	<0.01	<0.01	<0.01	<0.01	1.6	0.0002	<0.0001
Ti	-	-	-	-	-	-	0.01	0.015
V	-	-	-	-	-	-	0.01	0.01
Zn	<0.003	<0.02	<0.005	<0.02	<0.02	<0.02	0.005	0.002

Table 2

Neutron Fluence And Irradiation Temperature

For Magnesium And Aluminum Alloys

Composition	HFIR Axial Position	Axial Flux Ratio	Fluence x 10^{22} n/cm^2 Thermal	>0.2 Mev	>0.8 Mev	T,°C
	1	.465	1.9	1.4	1.0	
	2	.675	4.6	2.1	1.4	
Pure Mg	3	0.840	5.7	2.6	1.8	101.6
Mg/5.0 wt% Al/0.35 wt% Ce	4	0.950	6.5	2.9	2.0	114.2
Mg/3.0 wt% Al/0.19 wt% Ca	5	1.000	6.8	3.1	2.1	119.2
Mg/5.1 wt% Al/1.6 wt% Sn	6	0.983	6.7	3.0	2.0	122.5
Mg/5.2 wt% Al/0.20 wt% Ca	7	0.900	6.1	2.8	1.9	121.7
Mg/7.7 wt% Al	8	0.773	5.3	2.4	1.6	106.7
6063 Al	9	0.605	4.1	1.9	1.3	117.4
1100 Al	10	0.415	2.8	1.3	0.9	112.0

The alloys were irradiated as rods or tensile samples in position F-7 of the HFIR Target Bundle at ORNL from November 16, 1969, to October 15, 1970, for a total of 30,235 megawatts or 302.35 full power days. T°C, is the calculated irradiation temperature at the center of the sample.

Table 3

Density Changes In Irradiated Magnesium

And Aluminum Alloys

Alloy	Density Change ($\Delta\rho/\rho$, %)
Pure Magnesium	-10.6
Mg/7.7 wt% Al	-0.37
Mg/3.0 wt% Al/0.19 wt% Ca	-0.13
Mg/5.2 wt% Al/0.20 wt% Ca	-0.23
Mg/5.1 wt% Al/1.6 wt% Sn	-0.51
Mg/5.0 wt% Al/0.35 wt% Ce	-0.32
1100 Al (DPH=27)	-0.33
1100 Al (DPH=52)	-0.31
6063 Al* (DPH=30)	-0.22
6063 Al* (DPH=63)	-0.21
6063 Al* (DPH-83)	-0.22

* Varying degrees of precipitation hardening before irradiation had no apparent effect on swelling.

Table 4

Lattice Parameters And Unit Cell Volume

Changes For Magnesium Alloys

Alloy	a		c		$(\frac{\Delta V}{V})\%$**
	U*	I*	U	I	
Mg/3.0 wt% Al/0.19 wt% Ca	3.1988	3.2033	5.1928	5.2069	0.55
Mg/5.2 wt% Al/0.20 wt% Ca	3.1787	3.2049	5.1638	5.2001	2.31
Mg/5.0 wt% Al/0.35 wt% Ce	3.1857	3.2077	5.1716	5.2063	2.02
Mg/5.1 wt% Al/1.6 wt% Sn	3.1806	3.2025	5.1672	5.1955	1.90
Mg/7.7 wt% Al	3.1735	3.2036	5.1582	5.2045	2.74

* U is unirradiated, I is Irradiated

** V is unit cell volume $\sqrt{3}/2\ a^2c$.

Table 5

Mechanical Properties Of Magnesium And Aluminum Alloys

Alloy	Yield Strength (ksi)*		Ultimate Strength (ksi)		Elong. to Fracture (%)	
	(BI)*	(AI)*	(BI)	(AI)	(BI)	(AI)
High Purity Mg	6.2	10.3	20.8	13.7	11.5	1.6
Mg/7.7 wt% Al	28.4	40.5	44.0	52.4	10.8	1.8
Mg/3.0 wt% Al/0.19 wt% Ca	20.7	36.3	35.4	46.1	17.8	3.1
Mg/5.2 wt% Al/0.20 wt% Ca	22.4	38.1	37.6	39.0	14.5	0.3
Mg/5.1 wt% Al/1.6 wt% Sn	24.3	36.2	35.0	37.1	7.5	0.3
Mg/5.0 wt% Al/0.35 wt% Ce	24.9	32.9	38.7	42.5	12.2	2.1
1100 Al (DPH=27)	3.2	18.4	12.8	25.8	33.8	15.5
1100 Al (DPH=52)	20.6	26.3	23.0	29.6	11.4	9.8
6063 Al (DPH=30)	3.3	21.5	13.5	29.8	26.2	11.9
6063 Al (DPH=63)	18.6	26.9	25.7	34.8	12.0	9.0
6063 Al (DPH=83)	29.2	34.7	34.7	41.3	11.4	7.4

* ksi = pounds per square inch divided by 1000:

BI - Before Irradiation, AI - After Irradiation.

Table 6

Effects Of Irradiation On The Hardness Of Mg And Al Alloys

	Diamond Pyramid Hardness*	
	Before Irradiation	After Irradiation
Pure Mg	27	33
Mg/7.7 wt% Al	62	91
Mg/3.0 wt% Al/0.19 wt% Ca	50	85
Mg/5.2 wt% Al/0.20 wt% Ca	55	87
Mg/5.1 wt% Al/1.6 wt% Sn	54	86
Mg/5.0 wt% Al/0.35 wt% Ce	55	86
1100 Al	27	65
1100 Al	52	71
6063 Al	30	74
6063 Al	63	83
6063 Al	83	101

* 500 g load.

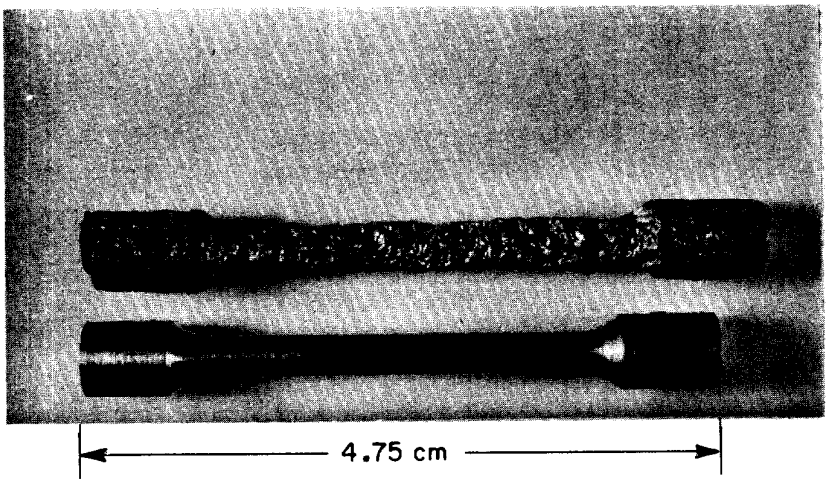

FIGURE 1. Comparison of irradiated pure magnesium with Mg/3.0 wt% Al/0.19 wt% Ca alloy. The pure magnesium suffered severe swelling and distortion due to voids and intergranular cavities [4]. The magnesium alloys suffered only minor changes in density.

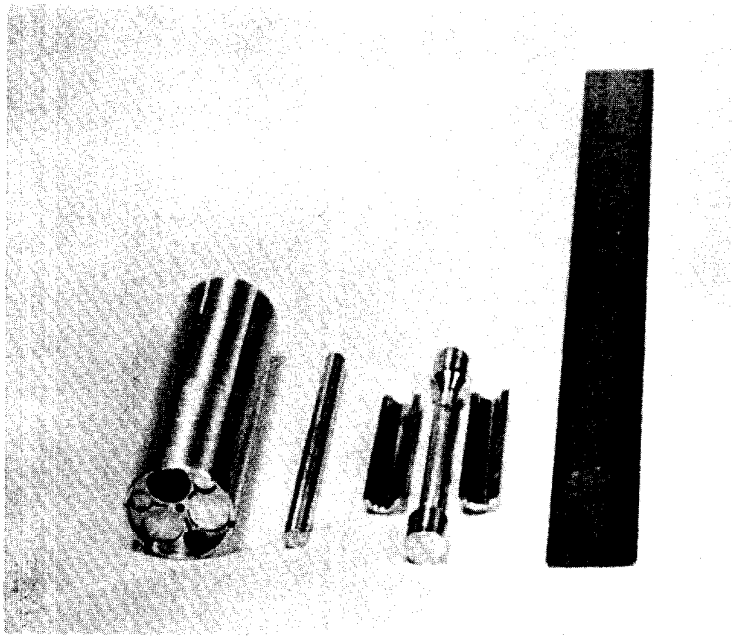

FIGURE 2. Specimen holder and specimens for irradiation experiments. Holder is of the same material as the specimens. The rods are 4.750 cm long x 0.318 cm diameter. The tensile specimens are 4.750 cm long x 0.556 cm diameter with a gauge length 2.858 cm long x 0.318 cm diameter. The gauge length is surrounded by a filler tube to provide good heat transfer. Specimens were irradiated in a sealed tube containing helium.

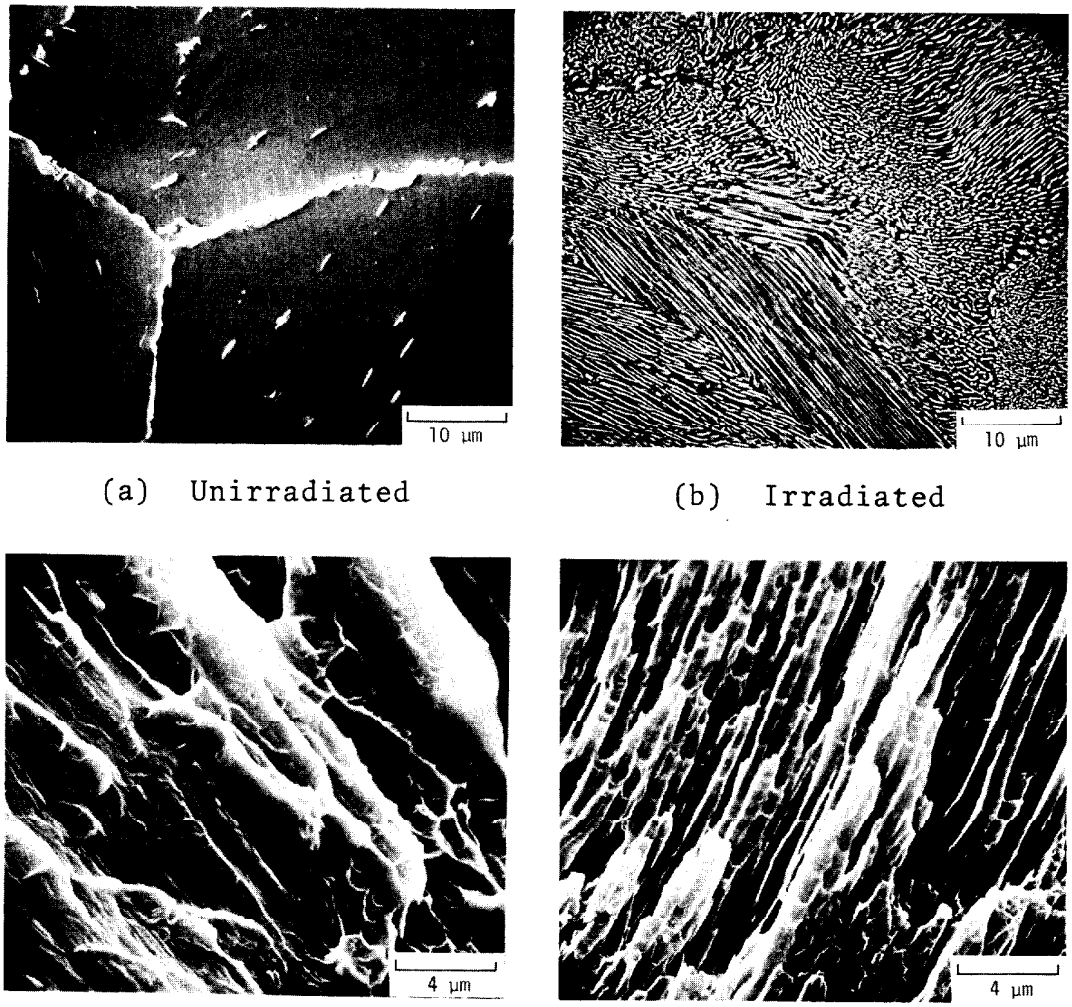

(a) Unirradiated (b) Irradiated

(c) Unirradiated (d) Irradiated

FIGURE 3. Microstructure and fracture structure of unirradiated and irradiated Mg/7.7 wt% Al alloy. Note that the fracture, (d), is occurring along the $Al_{12}Mg_{17}$ precipitate boundaries, (b).

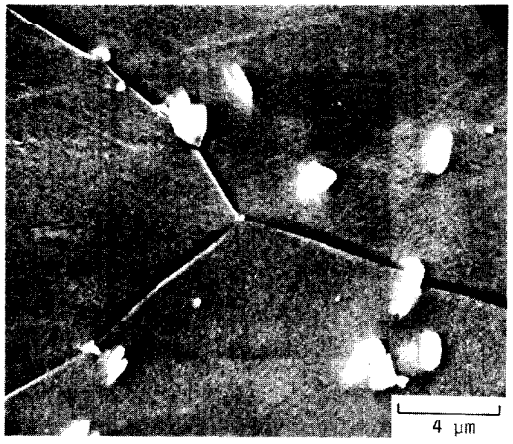

(a) Unirradiated

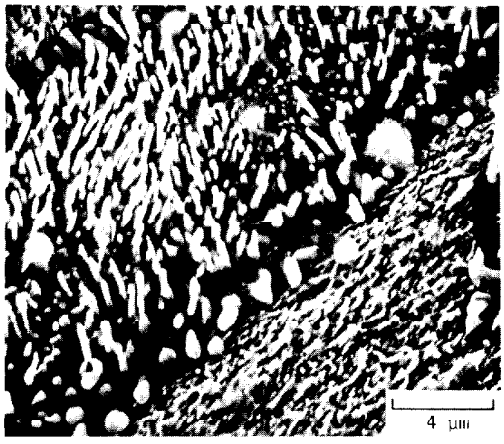

(b) Irradiated

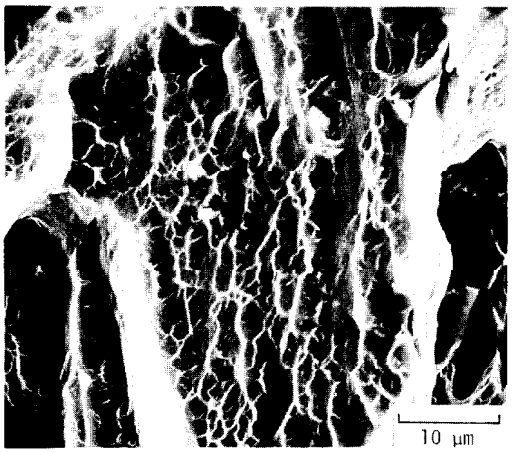

(c) Unirradiated

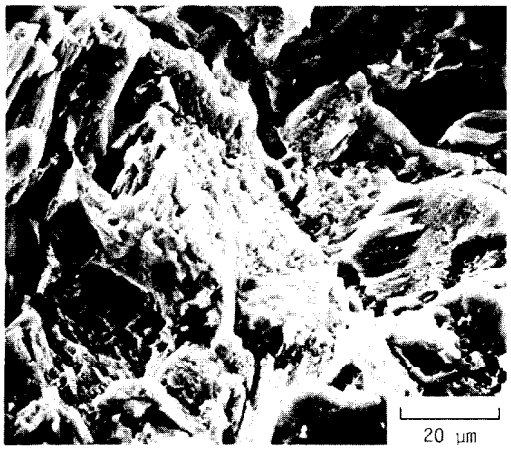

(d) Irradiated

FIGURE 4. Microstructure and fracture structure of unirradiated and irradited Mg/5 wt% Al/0.35 wt% Ce alloy. The fracture, (d), is occurring partly along participate boundaries and partly by cleavage due to mixed "cellular" and Widmanstätten structure, (b).

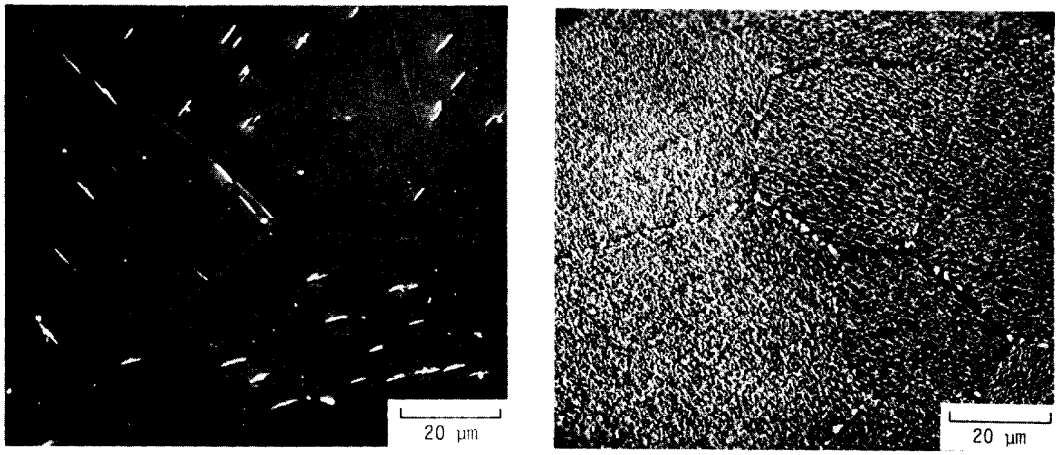

(a) Unirradiated (b) Irradiated

FIGURE 5. Microstructure of unirradiated and irradiated Mg/5.1 wt% Al/1.6 wt% Sn alloy. This alloy recrystallized, (b), to a finer grain size with $Al_{12}Mg_{17}$ Widmanstatten precipitates in grains and Mg_2Sn precipitates in grain boundaries.

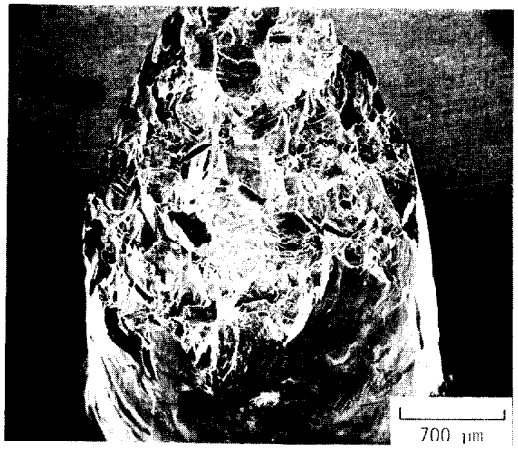

(a) Unirradiated

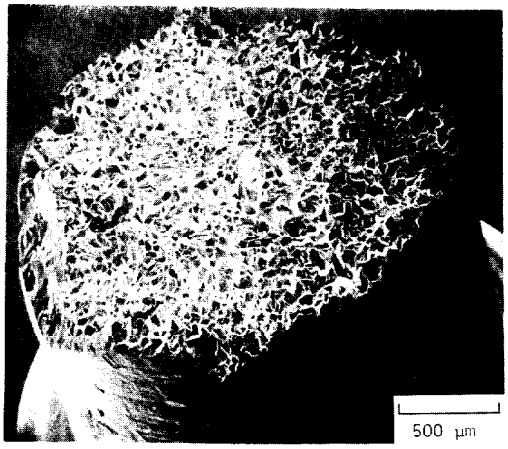

(b) Irradiated

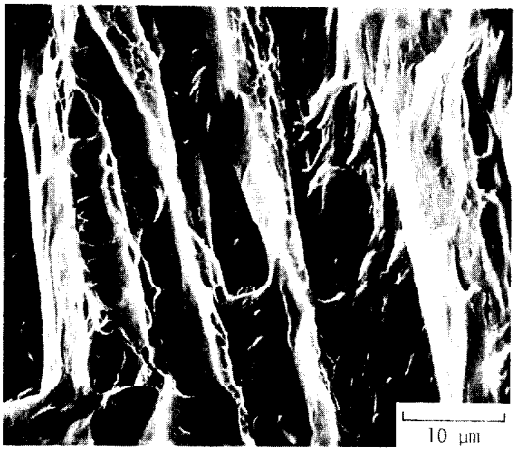

(c) Unirradiated

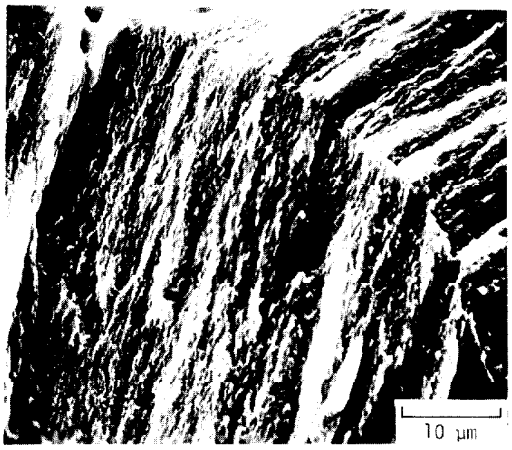

(d) Irradiated

FIGURE 6. Fracture structure of unirradiated and irradited Mg/5.1 wt% Al/1.6 wt% Sn alloy. Fracture in (b) is finer than (a) because of recrystallized grain structure. Many grains fractured by crystallographic cleavage, (d), on planes that contained the $Al_{12}Mg_{17}$ precipitates. The rough surface in (d) is due to holes equal to the size of the precipitates.

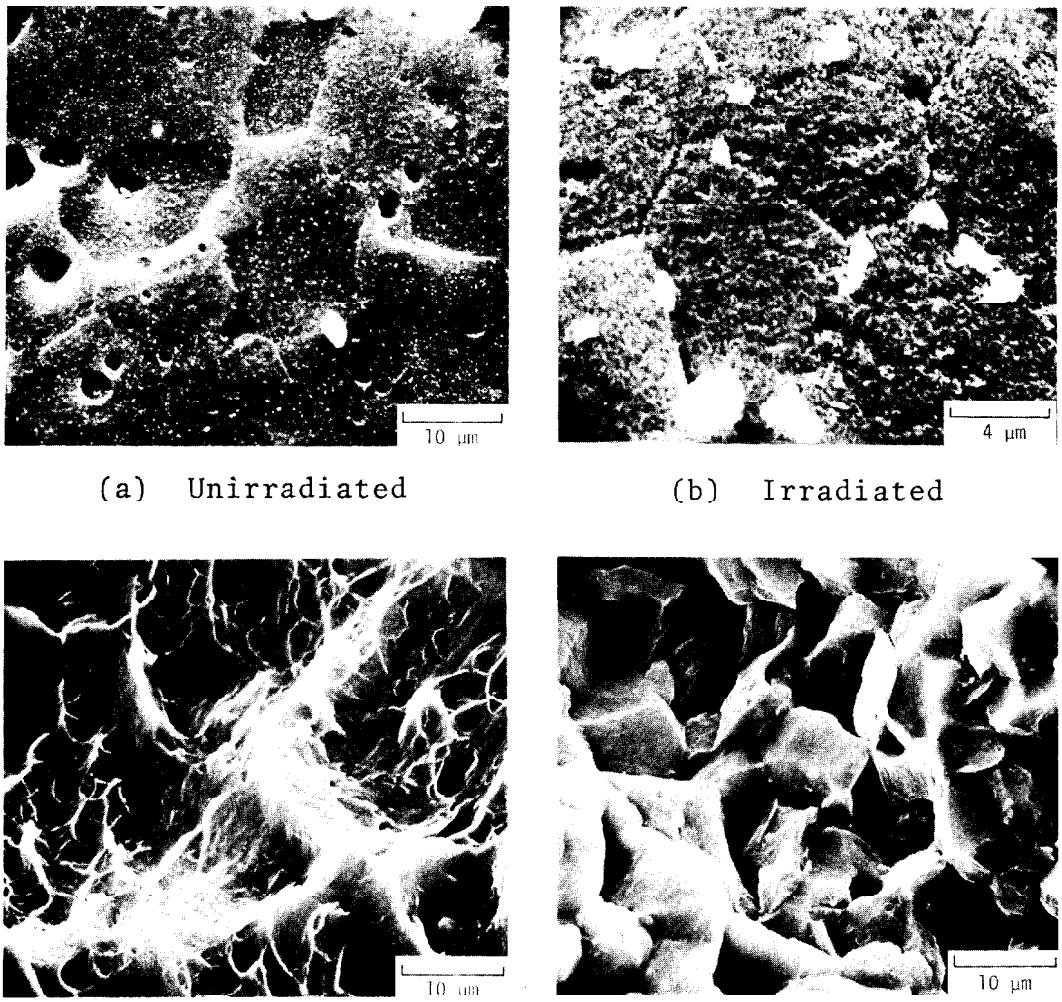

(a) Unirradiated (b) Irradiated

(c) Unirradiated (d) Irradiated

FIGURE 7. Microstructure and fracture structure of unirradiated and irradiated Mg/3.0 wt wt Al/0.19 wt% Ca. Note fine Al_2Ca precipitates in (a). Irradiation produced larger grain boundary precipitates, (b), which caused intergranular fracture, (d).

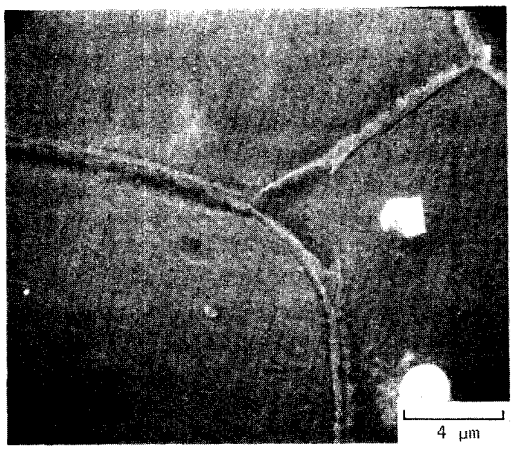

(a) Unirradiated

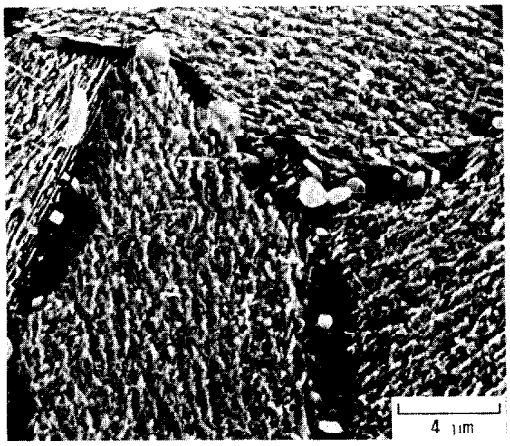

(b) Irradiated

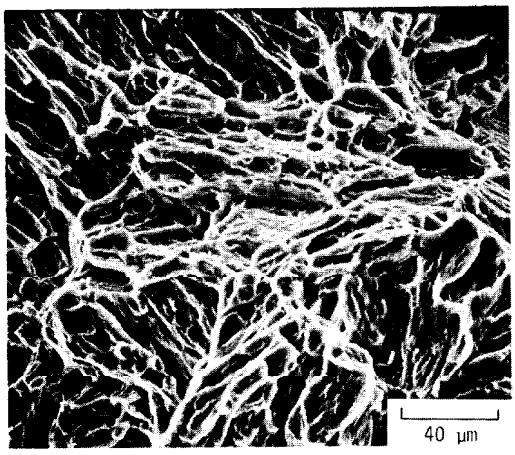

(c) Unirradiated

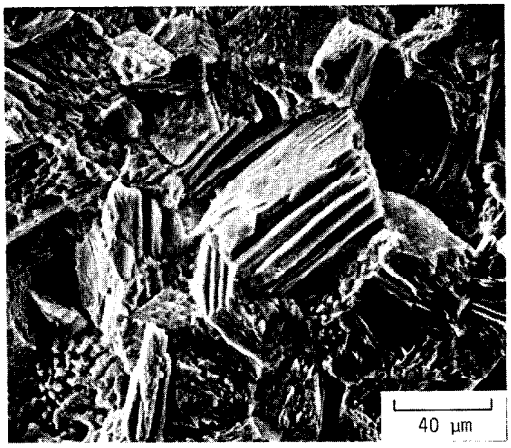

(d) Irradiated

FIGURE 8. Microstructure and fracture structure of unirradiated and irradiated Mg/5.2 wt% Al/0.20 wt% Ca. Widmanstätten precipitate structure of $Al_{12}Mg_{17}$ and grain boundary precipitates of Al_2Ca caused intergranular fracture and fracture by crystallographic cleavage.

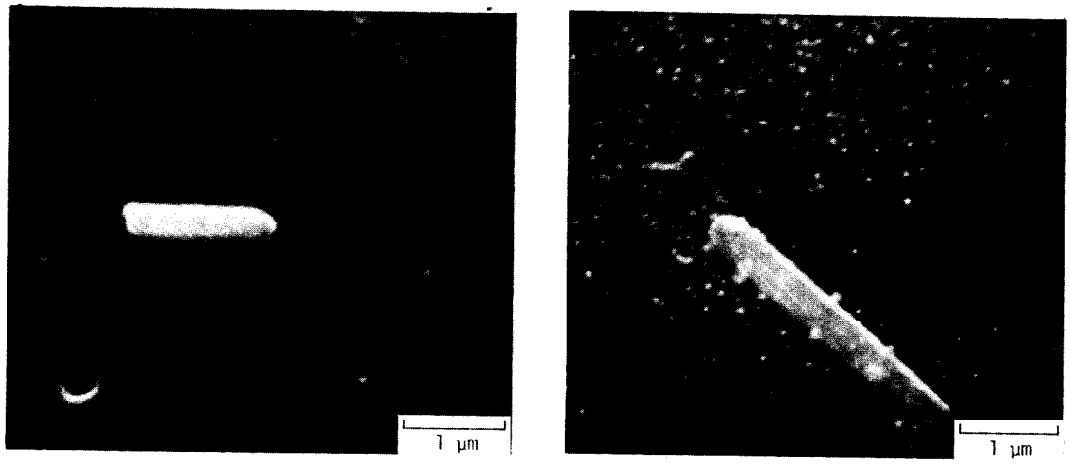

(a) Unirradiated (b) Irradiated

FIGURE 9. Precipitation of transmuted silicon in irradiated 6063 aluminum. The large rods are $Al_{12}Fe_3$ Si. The fine white particles in (b) are Si.

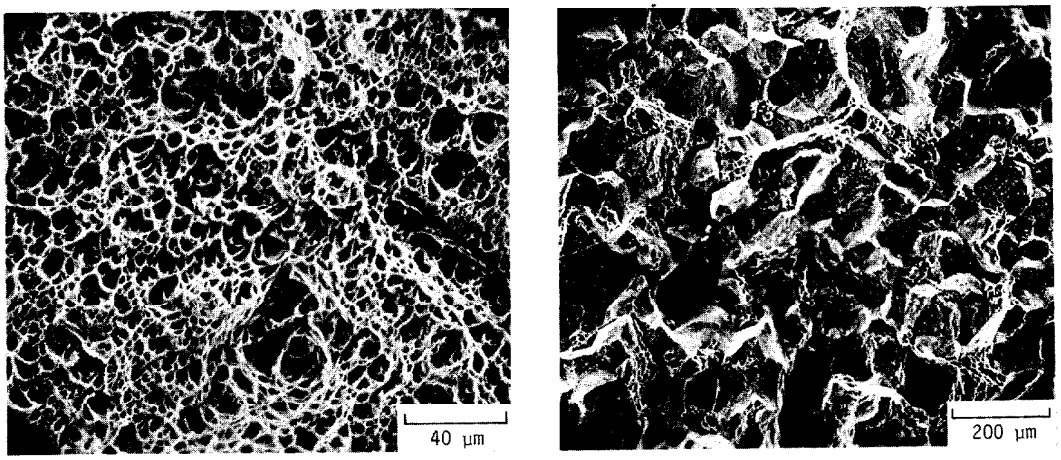

(a) Unirradiated (b) Irradiated

FIGURE 10. Fracture structure of unirradiated and irradiated 6063 aluminum. Fracture mode changed from typical cup and cone ductile rupture, (a), to partly intergranular rupture, (b).